

# Angle-integrated measurements of the $^{26}\text{Al}(d, n)^{27}\text{Si}$ reaction cross section: a probe of spectroscopic factors and astrophysical resonance strengths

A. Kankainen<sup>1,a</sup>, P.J. Woods<sup>1</sup>, F. Nunes<sup>2,3,4</sup>, C. Langer<sup>2,4,b</sup>, H. Schatz<sup>2,3,4</sup>, V. Bader<sup>2,3</sup>, T. Baugher<sup>2,c</sup>, D. Bazin<sup>2</sup>, B.A. Brown<sup>2,3,4</sup>, J. Browne<sup>2,3,4</sup>, D.T. Doherty<sup>1,d</sup>, A. Estrade<sup>1,e</sup>, A. Gade<sup>2,3</sup>, A. Kontos<sup>2</sup>, G. Lotay<sup>1,f</sup>, Z. Meisel<sup>2,3,4,g</sup>, F. Montes<sup>2,4</sup>, S. Noji<sup>2,h</sup>, G. Perdikakis<sup>4,5</sup>, J. Pereira<sup>2,4</sup>, F. Recchia<sup>2,i</sup>, T. Redpath<sup>5</sup>, R. Stroberg<sup>2,3</sup>, M. Scott<sup>2,3</sup>, D. Seweryniak<sup>6</sup>, J. Stevens<sup>2,4</sup>, D. Weisshaar<sup>2</sup>, K. Wimmer<sup>5</sup>, and R. Zegers<sup>2,3,4</sup>

<sup>1</sup> University of Edinburgh, Edinburgh EH9 3JZ, UK

<sup>2</sup> National Superconducting Cyclotron Laboratory, Michigan State University, East Lansing, MI 48824, USA

<sup>3</sup> Department of Physics and Astronomy, Michigan State University, East Lansing, MI 48824, USA

<sup>4</sup> JINA Center for the Evolution of the Elements, Michigan State University, East Lansing, MI 48824, USA

<sup>5</sup> Central Michigan University, Mount Pleasant, MI 48859, USA

<sup>6</sup> Argonne National Laboratory, Argonne, IL 60439, USA

Received: 12 October 2015

Published online: 14 January 2016

© The Author(s) 2016. This article is published with open access at Springerlink.com

Communicated by N. Kalantar-Nayestanaki

**Abstract.** Measurements of angle-integrated cross sections to discrete states in  $^{27}\text{Si}$  have been performed studying the  $^{26}\text{Al}(d, n)$  reaction in inverse kinematics by tagging states by their characteristic  $\gamma$ -decays using the GRETTINA array. Transfer reaction theory has been applied to derive spectroscopic factors for strong single-particle states below the proton threshold, and astrophysical resonances in the  $^{26}\text{Al}(p, \gamma)^{27}\text{Si}$  reaction. Comparisons are made between predictions of the shell model and known characteristics of the resonances. Overall very good agreement is obtained, indicating this method can be used to make estimates of resonance strengths for key reactions currently largely unconstrained by experiment.

## 1 Introduction

Hydrogen-burning reactions play a critical role in nuclear astrophysics. A major challenge has been to find ways to

<sup>a</sup> Present address: University of Jyväskylä, P.O. Box 35, FI-40014 University of Jyväskylä, Finland.

<sup>b</sup> Present address: Goethe-University Frankfurt a. M., D-60438 Frankfurt am Main, Germany.

<sup>c</sup> Present address: Rutgers, The State University of New Jersey, Piscataway, NJ 08854-8019, USA.

<sup>d</sup> Present address: University of York, Heslington, York YO10 5DD, UK.

<sup>e</sup> Present address: Central Michigan University, Mount Pleasant, MI 48859, USA.

<sup>f</sup> Present address: University of Surrey, Guildford GU2 7XH, UK.

<sup>g</sup> Present address: University of Notre Dame, Notre Dame, IN 46556, USA.

<sup>h</sup> Present address: Research Center for Nuclear Physics, Osaka University, Ibaraki, Osaka 567-0047, Japan.

<sup>i</sup> Present address: INFN LNL, 2 35020 Legnaro (Padua), Italy.

determine reaction rates at energies relevant for burning in the stellar environment, known as the Gamow window. A particular challenge is presented when the astrophysical reaction of interest involves a radioactive species. Here, even with the advent of new generation radioactive beam facilities, relatively few reactions have been measured directly at the energies of astrophysical interest. This is mainly due to limitations in the radioactive beam intensity and the sub-barrier nature of the reactions. Of particular importance are radiative proton-capture,  $(p, \gamma)$  reaction studies. The  $^{26}\text{Al}(p, \gamma)$  reaction represents an important example, since it destroys the cosmic  $\gamma$ -ray emitter  $^{26}\text{Al}$  in the interior of stars and decreases the amount of  $^{26}\text{Al}$  produced in these events. The reaction operates in the quiescent hydrogen burning phase of Wolf-Rayet stars prior to core collapse, and in the explosive burning conditions of novae [1].  $^{26}\text{Al}$  was the first cosmic  $\gamma$ -ray emitter to be discovered [2]. It showed nucleosynthesis is ongoing in our galaxy since its lifetime ( $\approx 1$  Myr) is short on cosmic time scales. Detailed observations by satellite missions of the distribution of  $^{26}\text{Al}$  flux across our galaxy by the CGRO, and more recently, INTEGRAL satellite missions [3], and

understanding its abundance relative to  $^{60}\text{Fe}$  [4, 5], present a challenge to nuclear astrophysics to reduce uncertainties in the  $^{26}\text{Al}(p, \gamma)$  reaction rate. In the present paper, we describe a new approach to estimating resonance strengths in proton capture reactions using  $(d, n)$  transfer reactions in inverse kinematics. The method is here first applied to the case of radioactive  $^{26}\text{Al}$ . The states of interest are identified with high resolution and efficiency by their characteristic  $\gamma$ -decay signatures, and measured in coincidence with forward-moving  $^{27}\text{Si}$  recoil ions produced in thick targets. Resonance strengths and spectroscopic factors are derived by comparing angle-integrated  $(d, n)$  cross sections for these states with theoretical calculations.

The lowest energy resonance strength measured directly for the  $^{26}\text{Al}(p, \gamma)^{27}\text{Si}$  reaction is at 189 keV [6, 7] (higher energy resonance strengths were reported in ref. [8]). The first resonance strength measurement was performed with a radioactive target [6], and more recently in inverse kinematics using a radioactive beam [7], with reasonable agreement obtained between the two approaches. The study of Ruiz *et al.* [7] using the DRAGON recoil separator represents a benchmark for such studies since a very high radioactive beam intensity ( $\approx 10^9$  pps) was available and only a few counts were observed over a running period of a few weeks. Lotay *et al.* [9, 10] used the Gammasphere germanium detector array [11, 12] to make spin and parity,  $J^\pi$ , assignments for  $\gamma$ -decaying states in  $^{27}\text{Si}$ , including states above the proton threshold energy ( $S_p = 7463.25(16)$  keV [13]). In particular, they reported that a state corresponding to a resonance energy of 127 keV had  $J^\pi = 9/2^+$  and therefore could destroy the  $5^+$  ground state of  $^{26}\text{Al}$  by  $l = 0$  proton capture in the low-temperature burning conditions of Wolf-Rayet stars ( $T \approx 0.05$  GK). The 127 keV resonance is, however, at too low an energy, and has therefore too low a cross section for a direct measurement to be presently feasible. A ( $^3\text{He}, d$ ) transfer reaction study on a  $^{26}\text{Al}$  target set a ( $l$ -dependent) limit on the spectroscopic factor  $C^2S$  for the 127 keV resonance [14], and inferred an upper limit on its strength (since  $\Gamma_\gamma \gg \Gamma_p$ , it is  $\Gamma_p$  that determines the resonance strength,  $\omega\gamma$ ). In the work of Lotay *et al.* [10], states in  $^{27}\text{Si}$  were paired with analog states in the stable mirror nucleus  $^{27}\text{Al}$ . Margerin *et al.* [15] and Pain *et al.* [16] studied the  $^{26}\text{Al}(d, p)$  differential cross sections in inverse kinematics to determine  $C^2S$  values for states in  $^{27}\text{Al}$ . The mirror assignments of Lotay *et al.* [9, 10] were then used to estimate resonance strengths for the analog states in  $^{27}\text{Si}$ . The  $C^2S(l = 0)$  value obtained for the analog of the 127 keV resonance indicated this resonance would dominate the destruction of  $^{26}\text{Al}$  in Wolf-Rayet stars. For the analog of the 189 keV resonance, thought to control destruction in the environment of novae, Margerin *et al.* [15] inferred the state was  $11/2^-$ , and therefore its resonance strength determined by  $l = 1$  proton capture, in contrast to ref. [9] where  $11/2^+$  is assigned.

The present paper presents an approach to estimating  $(p, \gamma)$  resonance strengths using the  $(d, n)$  transfer reaction mechanism to populate the states of interest, applied to the  $^{26}\text{Al}(p, \gamma)$  reaction. The  $(d, n)$  reaction has previously been used as a surrogate for the  $(p, \gamma)$  reaction [17] where

the  $^{26}\text{Al}$  radioactive beam was produced in-flight and an angle-integrated cross section was measured by detecting protons from the resonance of interest. In the present approach, using an in-flight  $^{26}\text{Al}$  beam, the angle-integrated  $(d, n)$  cross section is also measured. However, here the resonance of interest is identified by its characteristic  $\gamma$ -ray emission. For the states of interest where  $\Gamma_\gamma \gg \Gamma_p$ , the cross section when compared with theory, determines the  $C^2S$  for the state. This can then be used to obtain an estimate of the resonance strength. Critical to this approach is a prior knowledge of the  $\gamma$ -ray transitions from the astrophysical states of interest. In the present study, this uses the data from the Gammasphere study of  $^{27}\text{Si}$  by Lotay *et al.* [9, 10]. A central assumption in this methodology is that the proton-unbound states are fed directly in the  $(d, n)$  reaction mechanism and feeding by  $\gamma$ -decays from higher-lying proton-unbound states is suppressed by competition with proton decay. This might in principle give slight systematic overestimates of the spectroscopic factors and strengths. In contrast, the non-observation of weak  $\gamma$ -branches would tend to underestimate the cross section and derived spectroscopic factors and strengths. Overall therefore, one can expect to obtain good estimates of the spectroscopic factors and strengths with this methodology. This is important for determining proton capture reaction rates involving radioactive species. These rates can be uncertain by several orders of magnitude in astrophysical burning conditions due to the strengths being largely unconstrained by direct reaction measurements.

## 2 Experimental method

The experiment was performed at the National Superconducting Cyclotron Laboratory, Michigan State University. The 30 MeV/u  $^{26}\text{Al}^{13+}$  beam was produced in-flight via fragmentation reactions using a primary beam of 150 MeV/u, 112 pA  $^{36}\text{Ar}^{18+}$  ions to bombard a 1960 mg/cm<sup>2</sup> thick Be target. The A1900 high-resolution fragment separator [18] selected the ions of interest based on the momentum/charge,  $p/q$ , ratio after they had passed through a 600 mg/cm<sup>2</sup> thick Al wedge. The  $^{26}\text{Al}$  beam had a high purity (98(2)%) and an average intensity of  $8.1(4) \times 10^5$  particles per second. The fraction of the shorter-lived ( $T_{1/2} = 6.3$  s)  $0^+$  isomeric state of  $^{26}\text{Al}$  in the beam was determined prior to the experiment as 14.3(23)% by stopping the beam in a 5.1 mm thick Al sheet and observing the decay of the 511 keV  $\gamma$ -rays measured using GRETINA (Gamma-Ray Energy Tracking In-beam Nuclear Array) [19]. The attenuation of the 511 keV  $\gamma$ -rays was estimated using a GEANT4 simulation of the GRETINA setup [20]. The overall uncertainty in the integrated  $^{26}\text{Al}$  ground-state beam current was estimated as  $\pm 17\%$ .

In the main experiment, the  $^{26}\text{Al}$  beam impinged onto a 10.7(8) mg/cm<sup>2</sup> thick deuterated polyethylene target  $(\text{CD}_2)_n$  with the GRETINA detectors positioned at laboratory angles of  $58^\circ$  and  $90^\circ$ . Recoil products were identified with the S800 spectrograph [21] downstream of the

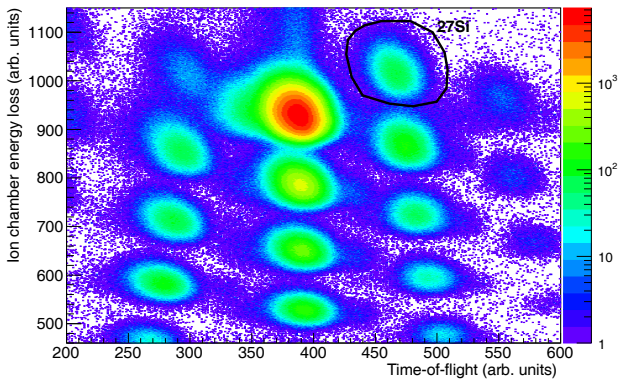


**Fig. 1.** (Color online) Particle identification spectrum of reaction products. The gate used as identification of  $^{27}\text{Si}$  reaction products is highlighted.

GRETINA setup. The S800 was run in focused mode in order to allow a large momentum acceptance. For  $^{27}\text{Si}^{14+}$  ions, an acceptance of 95.2(9)% at the S800 focal plane was determined. The data acquisition was triggered either by recoil- $\gamma$  coincidences between GRETINA and the first scintillator at the focal plane of the S800 or by scaled down ( $\times 1/6$ ) recoil singles events. Figure 1 shows recoil events at the focal plane of the S800 highlighting the  $^{27}\text{Si}$  ions of interest clearly separated from other recoil species. The GRETINA efficiency was calibrated with  $^{56}\text{Co}$ ,  $^{152}\text{Eu}$  and  $^{226}\text{Ra}$  sources. The in-beam efficiency, assuming isotropic emission in the frame of  $^{27}\text{Si}$  ions, was about 1.06(5) higher than the efficiency obtained with a stationary source based on simulations using the UCGretina GEANT4 simulation package [20]. To account for background from ( $d, n$ ) reactions on carbon in the target, measurements were also performed for an approximately equal duration with a 8.8(15) mg/cm<sup>2</sup> thick polyethylene target ( $\text{CH}_2$ )<sub>n</sub>. Figure 2 shows Doppler reconstructed  $\gamma$ -ray spectra in coincidence with  $^{27}\text{Si}$  recoils for obtained using the  $\text{CD}_2$  and  $\text{CH}_2$  targets, with the latter scaled to match the thickness and integrated beam on the  $\text{CD}_2$  target. The yield is significantly lower on the  $\text{CH}_2$  target, indicating that the dominant production of  $^{27}\text{Si}$  ions is associated with deuterium (the radiative capture cross section on protons is negligible at these energies). As expected, broadly speaking similar states are populated in  $^{27}\text{Si}$  by the ( $d, n$ ) stripping reaction on C nuclei and deuterium.

### 3 Results and discussion

We consider first the state at 7651.9(6) keV corresponding to the 188.7(6) keV resonance [9,10]. Two transitions were observed from this state at energies of 2373(2) and 3205(2) keV (see fig. 2.a). These energies are in good agreement with the two main transitions from this state reported by Lotay *et al.* at 2371.0(40) and 3204.1(1) keV [9]. Lotay *et al.* subsequently reported the further observation of two weaker transitions but these are not observed here [10]. In the direct study of the  $^{26}\text{Al}(p, \gamma)^{27}\text{Si}$  reaction by Vogelaar *et al.*, the 3204 keV transition was reported as the dominant branch

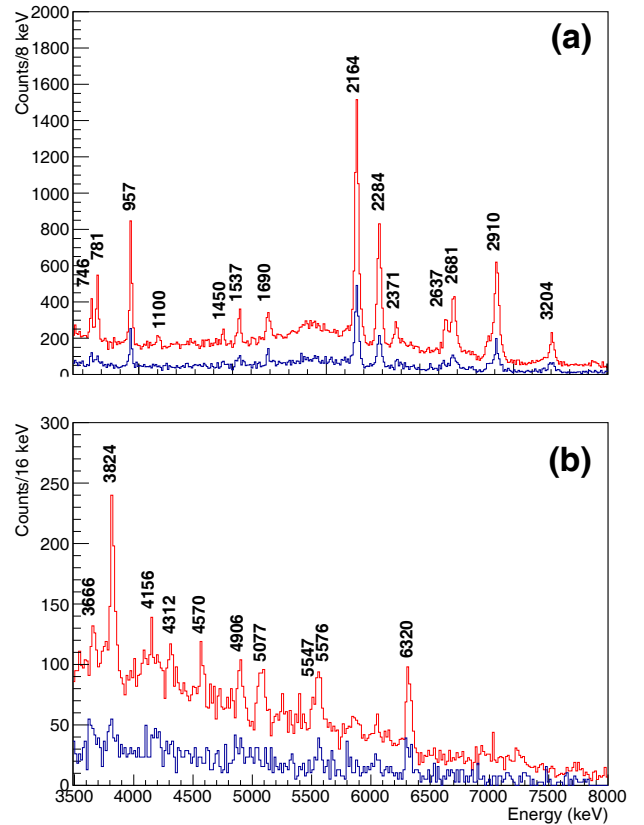


**Fig. 2.** (Color online) Doppler-reconstructed  $\gamma$ -ray spectrum in coincidence with  $^{27}\text{Si}$  recoils (in red) and a background spectrum scaled to similar conditions (in blue).

( $\approx 90\%$  [6]). Here, our measurements are consistent with a 86(14)% branch for the 3204 keV transition, and 14(9)% for the 2371 keV branch. The work of Lotay *et al.* [9,10] did not report on intensity or branching ratio measurements. The properties of the mirror analog state at 7948 keV in  $^{27}\text{Al}$  [22] suggest the two weaker branches can contribute at most  $\approx 10\%$ . In table 1, the ( $d, n$ ) cross-section value for the 7652 keV state in  $^{27}\text{Si}$  is calculated based on the two dominant transitions observed here.

We now consider the excited state at 7739.3(4) keV [9,10] corresponding to a resonance energy of 276.1(4) keV. This state was studied by Buchmann *et al.* [8], where a dominant  $\gamma$ -decay branch of 62(9)% was measured to the  $7/2^+$  state at 2164 keV with four much weaker branches also reported. Here we clearly observe in fig. 2.b a transition at 5575(6) keV corresponding to this dominant branch in agreement in energy with the energy of 5575.7(2) reported by Lotay *et al.* [9,10]. We also see some evidence for the next strongest transition at 2454 keV reported by Buchmann *et al.* as having a 12(4)% branch from the resonance. However, in deriving our ( $d, n$ ) cross-section value shown in table 1, only the dominant branch is used.

For the lower energy 126.9(9) keV resonance, corresponding to an excited state at 7590.1(9) [9,10] there are no direct capture measurements and no branching ratios known. The work of Lotay *et al.* [9,10] identified

**Table 1.** Experimental ( $\sigma_{exp}$ ) and theoretical ( $\sigma_{theor}$ ) cross sections and spectroscopic factors  $C^2S(d, n)$  determined in this work. Errors given for  $C^2S(d, n)$  are entirely estimated from experiment. The spectroscopic factors from ( $^3\text{He}, d$ ) [14] and ( $d, p$ ) measurements [15] and from the shell-model calculations (for positive parity states both USDA/USDB calculation predictions are shown) are listed for comparison assuming a single  $l$ -transfer. The ( $d, p$ ) values are assigned as analog states in the mirror nucleus  $^{27}\text{Al}$  [10, 15].

$E_x$ (keV)	$E_{res}$ (keV)	$J^\pi$	$l$	$\sigma_{exp}$ ( $\mu\text{b}$ )	$\sigma_{theor}$ ( $\mu\text{b}$ )	$C^2S(d, n)$	$C^2S(^3\text{He}, d)$	$C^2S(d, p)$	$C^2S_{SM}$
5547.3(1)		9/2 <sup>+</sup>	2	520(110)	850	0.61(13)			0.44/0.42
6734.0(2)		11/2 <sup>+</sup>	2	390(90)	1104	0.35(8)			0.50/0.50
7129.0(2)		13/2 <sup>+</sup>	2	630(130)	1262	0.5(1)			0.77/0.74
7590.1(9)	126.9(9)	9/2 <sup>+</sup>	0	$\leq 37$	375	$\leq 0.10$	$\leq 0.002$	0.0093(17)	0.011/0.017
			2	$\leq 37$	757	$\leq 0.05$	–	0.068(14)	0.053/0.052
7651.9(6)	188.7(6)	11/2 <sup>-</sup>	1	280(70)	1260	0.22(5)	0.16	0.14(3)	0.067
			3	280(70)	2517	0.11(3)	0.49	–	0.480
7739.3(4)	276.1(4)	9/2 <sup>+</sup>	0	70(30)	370	0.19(9)	0.087	–	0.019/0.011
			2	70(30)	746	0.10(5)	0.124	–	0.0092/0.011
		9/2 <sup>-</sup>	1	70(30)	982	0.07(4)	0.064	–	0.038
			3	70(30)	2070	0.035(16)	0.199	–	0.11

a number of  $\gamma$ -transitions from this state with a “high-intensity” transition at 5425.9(1) keV. We see no evidence for this high-intensity transition or any of the other weaker branches and set an upper limit (at  $2\sigma$  level) for the ( $d, n$ ) cross section to this state in table 1 assuming a 60(8)% branch for the 5425.9 keV transition based on measured decay branches from the 7806 keV state identified as the analog in  $^{27}\text{Al}$  [10, 22].

The theoretical cross sections shown in table 1 were computed within the finite-range adiabatic approximation [23]. This three-body method incorporates deuteron breakup and has been proven to provide a good description of the transfer process when compared to exact solutions of the three-body problem [24]. For the nucleon-target optical potentials we use CH89 [25] and for the  $NN$  interaction ref. [26]. In order to produce the desired  $p-^{26}\text{Al}$  final state, we use a central real Woods-Saxon potential with a radius  $r = 1.25$  fm, a diffuseness parameter  $a = 0.65$  fm, and a spin-orbit term with  $V_{so} = 6$  MeV and the same geometry as the central interaction. All states of astrophysical interest are resonances, however, for convenience, the depth of the  $p+^{26}\text{Al}$  interaction was adjusted to produce a state bound by  $E = 0.001$  MeV. We tested our bound state approximation by introducing a resonance at the exact experimental value, and constructing a bin wave function, averaging the resonance over the width. We found the total cross section to agree with that produced by the barely bound state  $E = 0.001$  MeV within 1%. The effective adiabatic potential was computed with TWOFNR [27] and the transfer calculations were performed with FRESKO [28]. There is uncertainty associated with the choice of single-particle parameters. A reduction of the radius parameter by 3% (to match the rms radius produced in state-of-the-art EDF calculations) produces changes in the total cross section of up to 5% for the states considered here. Based on a previous study [29], we estimate an error

up to 30% in our total cross-section calculations. Since the ground-state spin of  $^{26}\text{Al}$  is non-zero ( $5^+$ ), two different orbital-angular-momentum components can contribute to the total ( $d, n$ ) transfer cross section to a given state.

Theoretical spectroscopic factor values shown in table 1 were obtained from shell-model calculations. For the positive-parity states, we used the  $sd$ -shell model space with the USDA-cdnpn and USDB-cdnpn Hamiltonians. USDA/USDB refer to the isospin conserving interactions obtained in ref. [30], and “cdnpn” refers to the addition of the Coulomb, charge-dependent and charge-asymmetric nuclear Hamiltonian obtained by Ormand and Brown in a proton-neutron basis [31]. These Hamiltonians have been used for a series of ( $p, \gamma$ ) rate calculations in the  $sd$  shell [32–36]. For the negative-parity states we use the  $1\hbar\omega$  basis introduced in ref. [36] that allows for the excitation of one nucleon from  $0p$  to  $1s-0d$  or the excitation of one nucleon from  $1s-0d$  to  $0p-1f$ . The calculations were carried out with the NuShellX code [37]. We use the WBP Hamiltonian from ref. [38] that was designed to reproduce the energies of  $1\hbar\omega$  states for  $A = 10-20$ . WBP also contains the  $sd-pf$  Hamiltonian from [39] that was designed to reproduce energies of  $1\hbar\omega$  states in nuclei with  $A = 35-43$ . The  $0p_{1/2}$  single-particle energies were adjusted to reproduce the excitation energy of the lowest  $1/2^-$  states in  $^{27}\text{Si}$  and  $^{27}\text{Al}$ . The  $0f_{7/2}$  and  $1p_{3/2}$  single-particle energies were adjusted to reproduce the excitation energies of the lowest  $7/2^-$  and  $3/2^-$  states in  $^{29}\text{Si}$  and  $^{29}\text{P}$ . For the  $0p_{3/2}$ ,  $1p_{1/2}$  and  $0f_{5/2}$  energies we used typical spin-orbit splittings of about 6 MeV from their partners.

In order to test our experimental approach, we explored three states at 5547, 6734 and 7129 keV situated below the proton threshold energy and predicted by the shell model to have high single-particle strengths. These states should be produced directly in the ( $d, n$ ) reaction with a relatively small contribution from feeding by  $\gamma$ -

transitions from higher-lying states. In these cases, cross sections were derived based on the identification of dominant transitions from the states of interest (1100, 2637 and 5547 keV transitions for the 5547 keV level, 1450, 3824 and 4570 keV transitions for the 6734 keV state, and a 2681 keV transition for the state at 7129 keV, see fig. 2). These cross sections are shown in table 1 and compared to the theoretical cross-section calculations for  $l = 2$  transfer, predicted to be the dominant component for these states. The ratio of these values is then used to derive a spectroscopic factor,  $C^2S$ , for each state, which is compared with shell-model predictions in table 1. It can be seen from table 1 that there is excellent agreement between experiment and theory for these strong single-particle states, giving confidence in our methodology.

Considering the  $11/2^-$  state at 7652 keV, corresponding to the resonance at 189 keV, the present data agree within errors, but give a relatively higher value, compared with the  $C^2S(l = 1)$  value obtained for the state in the ( $^3\text{He}, d$ ) study [14], and the study of the mirror analog state in the ( $d, p$ ) reaction [15], assuming pure  $l = 1$  transfer (see table 1). The weighted mean value of the resonance strength obtained from the two direct measurements of  $45^{+19}_{-17} \mu\text{eV}$  [6,7] implies  $C^2S(l = 1) \approx 0.1$  (it is the  $l = 1$  contribution that determines  $\omega\gamma$ ). This would be compatible with an  $l = 3$  contribution to the cross section with  $C^2S(l = 3) \approx 0.05$ . The shell-model prediction for the  $C^2S(l = 1)$  component is smaller than observed but in reasonable agreement with experiment. However, the dominant  $l = 3$  component of the wave function predicted by the shell-model calculation is significantly higher than allowed by experiment.

The state at 7739 keV, corresponding to a resonance at 276 keV was assigned as  $9/2^+$  by Lotay *et al.* [9], with the spin being based on measured angular distributions, whereas the parity was based on matching characteristics with the analog state in the mirror nucleus  $^{27}\text{Al}$ . The measured resonance strength of 3.8(1) meV [8] requires  $C^2S(l = 0) \approx 0.02$ . Using the present data this would require a dominant  $l = 2$  component in the ( $d, n$ ) transfer cross-section data with a value  $C^2S(l = 2) \approx 0.1$ . This would be consistent with the value obtained by Vogelaar *et al.* in the ( $^3\text{He}, d$ ) study assuming pure  $l = 2$  transfer [14]. However, this is inconsistent with the shell-model calculation which predicts approximately equal values for  $C^2S(l = 0) \approx 0.01$  and  $C^2S(l = 2) \approx 0.01$ . Alternately, the cross section we measure here gives a derived  $C^2S(l = 1)$  value in excellent agreement with the ( $^3\text{He}, d$ ) study, assuming pure  $l = 1$  transfer, and is also consistent with the measured resonance strength (which implies  $C^2S \approx 0.07$ ). The  $C^2S(l = 1)$  shell model value is in good agreement with both the ( $d, n$ ) and ( $^3\text{He}, d$ ) experiments assuming dominant  $l = 1$  transfer. However, a possible  $l = 3$  contribution to the wave function must be significantly lower than predicted by the shell model and smaller than the  $l = 1$  component to describe the ( $d, n$ ) data.

The upper limit on the ( $d, n$ ) cross section to the 7590 keV state gives a  $C^2S(l = 0)$  limit consistent with the limit obtained in the ( $^3\text{He}, d$ ) study [14] and the val-

ues deduced from the ( $d, p$ ) experiments [16,15]. The integrated cross section is expected to be dominated by  $l = 2$  transfer. The upper limit value of  $C^2S(l = 2) \approx 0.05$  (at the  $2\sigma$  level) is only just compatible with the ( $d, p$ ) data of ref. [15] which gives a resonance strength of  $0.025(5) \mu\text{eV}$ .

Overall, in considering the astrophysical resonances, we can say that the method is able to reproduce very well the characteristics of the resonances, with reasonable agreement obtained with shell-model predictions of the  $C^2S$  values. There is some evidence that  $l = 3$  components are overestimated by shell-model calculations for negative-parity states. For theoretical negative-parity states the theory is not so reliable in being able to compare with specific states of a given  $J^\pi$  and excitation energy. For example, the shell model predicts three  $11/2^-$  states at 7.63, 7.90 and 8.33 MeV. The comparison of the spectroscopic factors for the 7.74 MeV state in table 1 is made with the 7.63 MeV state prediction, however, the 7.90 and 8.33 MeV states are predicted to have smaller  $C^2S(l = 3)$  components (0.02 and 0.07, respectively) that are more compatible with experiment. This would then imply that there is mixing between these theoretical states. For the positive-parity sub-threshold states with very strong single-particle amplitudes excellent agreement is obtained. This then gives confidence in applying this method to important astrophysical reactions where no direct measurements are currently possible, and resonance strengths are completely unconstrained by experiment. For example, the  $^{30}\text{P}(p, \gamma)$  reaction cannot be measured directly because of the unavailability of radioactive beams of sufficient intensity at the required energy. This reaction is important for understanding the elemental abundances of novae ejecta and isotope ratios in pre-solar grains [40]. In such cases one can determine which are the critical strong resonances (when combined with spectroscopic data [40]), and then get the first estimates of the resonance strength values. There remains some ambiguity when the beam species has non-zero ground-state spin since two  $l$ -amplitudes can contribute for a state of given parity, with the low  $l$ -value being the critical one for determining the resonance strength. However, for certain resonances the low  $l$ -transfer component will be dominant and, from comparisons with theory, reliable estimates of the strength will be feasible. Furthermore, there are a number of cases where the radioactive species of interest is an even-even nucleus with a  $0^+$  ground-state. In this case there is only one  $l$ -contribution to the reaction cross section.

In summary, we have measured the  $^{26}\text{Al}(d, n)$  angle-integrated reaction cross section to discrete states in  $^{27}\text{Si}$  using characteristic  $\gamma$ -rays to tag the states of interest. We have then applied reaction theory to derive spectroscopic factors for both astrophysical resonances and strong single-particle states below the proton threshold. The results agree well with both shell-model predictions and with previously known characteristics of the astrophysical resonances. This then provides a potentially powerful new approach to address important astrophysical ( $p, \gamma$ ) reactions where there is little or no direct experimental information.

The Edinburgh group is grateful for the support from the STFC grants. AK acknowledges the support from the Academy of Finland under project No. 275389. This work was supported by the National Science Foundation under Grant No. PHY-1403906. This research was sponsored in part by the National Nuclear Security Administration under the Stewardship Science Academic Alliance program through the DOE cooperative agreement DE-FG52-08NA28552. We also acknowledge support by the National Science Foundation under Grant No. PHY-1430152 (JINA Center for the Evolution of the Elements). GRETINA was funded by the US DOE Office of Science. Operation of the array at NSCL is supported by the NSF under Cooperative Agreement PHY-1102511(NSCL) and by the DOE under Grant No. DE-AC02-05CH11231(LBNL). We thank L. Riley for providing us the UCGretina GEANT4 code.

**Open Access** This is an open access article distributed under the terms of the Creative Commons Attribution License (<http://creativecommons.org/licenses/by/4.0>), which permits unrestricted use, distribution, and reproduction in any medium, provided the original work is properly cited.

## References

1. C. Iliadis *et al.*, *Astrophys. J. Suppl. Ser.* **142**, 105 (2002).
2. W.A. Mahoney, J.C. Ling, A.S. Jacobson, R.E. Lingenfelter, *Astrophys. J.* **262**, 742 (1982).
3. R. Diehl *et al.*, *Nature* **439**, 45 (2006).
4. S. Woosley, A. Heger, *Phys. Rep.* **442**, 269 (2007) The Hans Bethe Centennial Volume 1906–2006.
5. T. Rauscher, A. Heger, R.D. Hoffman, S.E. Woosley, *Astrophys. J.* **576**, 323 (2002).
6. R.B. Vogelaar, PhD thesis, California Institute of Technology, 1989.
7. C. Ruiz *et al.*, *Phys. Rev. Lett.* **96**, 252501 (2006).
8. L. Buchmann *et al.*, *Nucl. Phys. A* **415**, 93 (1984).
9. G. Lotay *et al.*, *Phys. Rev. Lett.* **102**, 162502 (2009).
10. G. Lotay *et al.*, *Phys. Rev. C* **84**, 035802 (2011).
11. I.-Y. Lee, *Nucl. Phys. A* **520**, c641 (1990) Nuclear Structure in the Nineties.
12. R.V.F. Janssens, F.S. Stephens, *Nucl. Phys. News Int.* **6**, 9 (1996).
13. M. Wang *et al.*, *Chin. Phys. C* **36**, 1603 (2012).
14. R.B. Vogelaar *et al.*, *Phys. Rev. C* **53**, 1945 (1996).
15. V. Margerin *et al.*, *Phys. Rev. Lett.* **115**, 062701 (2015).
16. S.D. Pain *et al.*, *Phys. Rev. Lett.* **114**, 212501 (2015).
17. P.N. Peplowski *et al.*, *Phys. Rev. C* **79**, 032801 (2009).
18. D. Morrissey *et al.*, *Nucl. Instrum. Methods Phys. Res. B* **204**, 90 (2003) 14th International Conference on Electromagnetic Isotope Separators and Techniques Related to their Applications.
19. S. Paschalis *et al.*, *Nucl. Instrum. Methods Phys. Res. A* **709**, 44 (2013).
20. L.A. Riley, 2014, UCGretina GEANT4, Ursinus College, unpublished.
21. D. Bazin *et al.*, *Nucl. Instrum. Methods Phys. Res. B* **204**, 629 (2003) 14th International Conference on Electromagnetic Isotope Separators and Techniques Related to their Applications.
22. M.S. Basunia, *Nucl. Data Sheets* **112**, 1875 (2011).
23. R.C. Johnson, P.C. Tandy, *Nucl. Phys. A* **235**, 56 (1974).
24. F.M. Nunes, A. Deltuva, *Phys. Rev. C* **84**, 034607 (2011).
25. R.L. Varner *et al.*, *Phys. Rep.* **201**, 57 (1991).
26. R.V. Reid, *Ann. Phys.* **50**, 411 (1968).
27. M.T.J. Tostevin, M. Igarashi, N. Kishida, University of Surrey modified version of the code TWOFNR, private communication.
28. I. Thompson, *Comput. Phys. Rep.* **7**, 167 (1988).
29. F.M. Nunes, A. Deltuva, J. Hong, *Phys. Rev. C* **83**, 034610 (2011).
30. B.A. Brown, W.A. Richter, *Phys. Rev. C* **74**, 034315 (2006).
31. W. Ormand, B. Brown, *Nucl. Phys. A* **491**, 1 (1989).
32. W.A. Richter, B.A. Brown, A. Signoracci, M. Wiescher, *Phys. Rev. C* **83**, 065803 (2011).
33. W.A. Richter, B.A. Brown, A. Signoracci, M. Wiescher, *Phys. Rev. C* **84**, 059802 (2011).
34. W.A. Richter, B.A. Brown, *Phys. Rev. C* **85**, 045806 (2012).
35. W.A. Richter, B.A. Brown, *Phys. Rev. C* **87**, 065803 (2013).
36. B.A. Brown, W.A. Richter, C. Wrede, *Phys. Rev. C* **89**, 062801 (2014).
37. B. Brown, W. Rae, *Nucl. Data Sheets* **120**, 115 (2014).
38. E.K. Warburton, B.A. Brown, *Phys. Rev. C* **46**, 923 (1992).
39. E.K. Warburton, J.A. Becker, B.A. Brown, *Phys. Rev. C* **41**, 1147 (1990).
40. D.T. Doherty *et al.*, *Phys. Rev. Lett.* **108**, 262502 (2012).